# Some Studies of Free-Surface Mercury Magnetohydrodynamics*

R. A. ALPHER, H. HURWITZ, JR., R. H. JOHNSON, AND D. R. WHITE

*General Electric Research Laboratory, Schenectady, New York*

## INTRODUCTION

THE investigations described had their origin in a suggestion by a colleague[1] that one ought to consider the possibility of a "magnetohydraulic" analogy. The proposition was to modify a "water table"[2] as used to study the conventional hydraulic analogy by employing a conducting fluid flowing through a transverse magnetic field. Accordingly a device employing mercury was constructed and placed in operation about a year ago.[3] In the course of our studies with and of the mercury table we have considered some shallow-liquid magnetohydrodynamic flows, surface wave motions, and rotating flows. However, we do not report here any experiments in which the mercury table has been used as an analog device in the sense of the conventional water table. Much of the work done thus far and reported here is still on a qualitative basis.

Free-surface magnetohydrodynamic phenomena have also been considered by Donaldson,[4] Donaldson and Golden,[4] Fraenkel,[5] Lundquist,[6] and Shirokov.[7] Fraenkel's work, in particular, is a penetrating discussion of many related shallow-liquid magnetohydrodynamic problems, including some of the wave-motion analysis included in the present paper. Lehnert[8] has reviewed or referred to much of the previous work on magnetohydrodynamic studies using liquid metals.

## DESCRIPTION OF THE MERCURY TABLE

The mercury table illustrated in Fig. 1 is patterned after a conventional water table. A shallow layer of mercury (typically $\frac{1}{2}$ to 1 cm deep) flows with a free surface through a relatively wide channel (typically 10 or 15 cm) between the poles of a large electromagnet. Flows with velocities up to a meter per second have been studied. The channel can be tilted or run with a depth gradient to overcome friction. The correction needed is very slight. Flow depth and velocity are controlled by a variable efflux from an upstream reservoir—the control is an adjustable bottom slot. The flow is spread to be smooth and to fill the channel by traversing a convergent-divergent section before entering the field. After passing through the transverse magnetic field the mercury drops into a sump where it is cooled and whence it is recirculated to the reservoir by a centrifugal pump—a water pump with its impeller cut down to handle mercury. The basic channel is Lucite to which side walls and bottom regions of desired geometry and conductivity can be fastened. The field is provided by a water-cooled magnet having 61-cm diam polepieces with a 10.25-cm gap. The power supply permits continuous operation up to 4200 gauss. Satisfactory uniformity obtains over a 50-cm region.

Before considering the several phenomena studied, let us develop the equations of flow in the channel.

## CHANNEL FLOW EQUATIONS

Consider steady-state shallow flow in the $x$ direction of an incompressible fluid with $z$ the depth coordinate as well as the direction of the uniform applied field. The channel is considered to be infinite in the $y$ direction. If

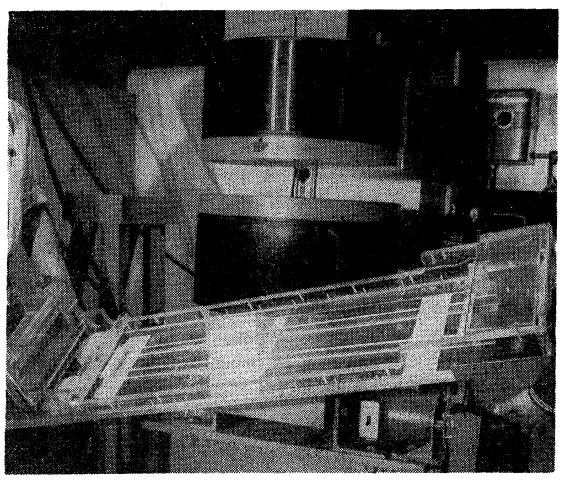

FIG. 1. Free-surface mercury channel is shown outside of the magnet gap for greater visibility. Copper strip and disk shown were used in experiments described in this paper.

* Portions of this work were supported by the Ballistic Missile Division, U. S. Air Force.

[1] A. J. Nerad (private communication).

[2] There is a considerable literature on the hydraulic analogy and water tables. See for example, the article by A. H. Shapiro, in *Princeton Series on High Speed Aerodynamics and Jet Propulsion* (Princeton University Press, Princeton, New Jersey, 1954), No. H, 1, Vol. IX; J. J. Stoker, *Water Waves* (Interscience Publishers, Inc., New York, 1958).

[3] R. A. Alpher and R. H. Johnson, Bull. Am. Phys. Soc. Ser. II, 4, 282 (1959). Such a device was suggested independently by C. duP. Donaldson and L. H. Fraenkel.

[4] C. duP. Donaldson, in *Heat Transfer and Fluid Mechanics Institute* (Stanford University Press, Stanford, California, 1959), p. 55. Also C. duP. Donaldson and K. I. Golden (unpublished).

[5] L. H. Fraenkel, J. Fluid Mech. 7, 81 (1960).

[6] B. Lundquist, Arkiv Fysik 5, 297 (1952).

[7] M. F. Shirokov, Soviet Phys. JETP 6, 50 (1958).

[8] B. Lehnert, *Electromagnetic Phenomena in Cosmical Physics*, Intern. Astron. Union Symp. (Cambridge University Press, New York, 1958), p. 50.

changes in the channel depth $h$ are taken to be small, then the continuity equation reduces to that for an incompressible fluid, viz.,

$$\nabla\cdot(h\mathbf{u})\cong\nabla\cdot\mathbf{u}=0. \tag{1}$$

It is supposed that the total field $\mathbf{H}$ and velocity $\mathbf{u}$ are functions of $z$ only, and that one may neglect free charge and displacement currents. If now vertical accelerations of the fluid be neglected, it then can be shown that the pressure gradient is constant in the flow direction, and the magnetohydrodynamic equations reduce to the following differential equation for the velocity $u$[9,10]:

$$d^3u/dz^3=(M^2/h^2)du/dz, \tag{2}$$

where the Hartmann number is defined as

$$M=(\mu Hh/c)(\sigma/\rho\nu)^{\frac{1}{2}},$$

where $H$ is in gauss, $\sigma$ is in esu, and the characteristic dimension $h$, in cm, is taken to be the channel depth. The solution of Eq. (2) which gives $u=0$ at $z=0$, and $u=u_0$, the surface velocity, at $z=h$, can be written as

$$u=u_0\frac{\cosh M}{(\cosh M)-1}\left[1-\frac{\cosh M(1-z/h)}{\cosh M}\right]. \tag{3}$$

For large Hartmann number, Eq. (3) reduces to

$$u\cong u_0[1-\exp(-Mz/h)]. \tag{4}$$

As with flow in a closed rectangular or circular channel[9–11] viscous effects are compressed into a very thin boundary layer—an exponential boundary layer at large Hartmann number. The flow as considered is one-dimensional, i.e., neither $u$ nor the boundary layer thickness vary in the flow direction. For an applied field of 4 kgauss and a depth of 1 cm, $M$ is 103.6, so that Eq. (4) predicts a very thin boundary layer indeed. Since by far the bulk of the flow is sluglike, i.e., at a uniform velocity, it would appear that flows at large Hartmann number might be approximated as inviscid flows. However, if the channel bottom is nonconducting the current flow through the Hartmann layer plays a significant role in determining the damping. This is discussed later in connection with rotating flows. We have not considered the boundary layer developed on the confining channel walls which are parallel to the applied field. The work of Shercliff[10] on closed channels suggests that these boundary layers are very curious as well as being very thin and we consider only flows in which the channel is quite wide compared to the fluid depth.

The velocity profile, Eq. (3), does not depend on whether the channel is insulating or conducting, although the pressure gradient to maintain a given $u_0$ certainly does. Moreover the induced electric and magnetic fields and the current density also depend on the bottom conductivity. Let us define

$$R=\sigma_b h_b/(\sigma_f h_f), \tag{5}$$

where $\sigma$ and $h$ are conductivity and thickness or depth, respectively, and the subscripts $b$ and $f$ refer to the channel bottom and to the fluid, respectively. Thus $R=0$ defines an insulated channel, and $R=\infty$ a channel bottom of infinite conductivity. A straightforward application of electromagnetic boundary conditions leads to the following for $E$, $H$, and current density per unit channel length, $j$, with $u_0'=u_0\times\cosh M/[(\cosh M)-1]$:

$$(E_y)_f=\frac{u_0'B_z}{c(1+R)}\left(1-\frac{1}{M}\tanh M\right)=(E_y)_b, \tag{6}$$

$$(E_x)_f=(E_z)_f=(E_x)_b=(E_z)_b=0, \tag{7}$$

$$(H_x)_f=\frac{4\pi\sigma_f}{c}\left\{\left[(E_y)_f-\frac{u_0'B_z}{c}\right](z-h)-\frac{u_0'B_z}{c}\frac{h}{M}\frac{\sinh M(1-z/h)}{\cosh M}\right\}, \tag{8}$$

$$(H_x)_b=\frac{4\pi J_f}{ch_b}(z+h_b), \tag{9}$$

$$(H_y)_f=(H_z)_f=(H_y)_b=(H_z)_b=0, \tag{10}$$

$$(j_y)_f=\sigma_f[(E_y)_f-uB_z/c], \tag{11}$$

$$(j_y)_b=\sigma_b(E_y)_b=J_b/h_b, \tag{12}$$

$$(j_x)_f=(j_z)_f=(j_x)_b=(j_z)_b=0, \tag{13}$$

where we have located $z=0$ at the interface between fluid and bottom and have required that the total current $J$ (per unit length of channel), i.e., current in the fluid plus that in the bottom, vanish. The quantities $J_f$ and $J_b$ are the total currents in the fluid and bottom. It follows from Eqs. (6)–(13) and the equations of motion that the pressure gradient may be written as

$$\frac{1}{\rho}\frac{\partial p}{\partial x}=-\frac{\sigma_f B_z^2 u_0'}{\rho c^2}\left(\frac{R}{1+R}+\frac{1}{1+R}\frac{1}{M}\tanh M\right). \tag{14}$$

If $M$ is very large, Eqs. (6)–(14) reduce to what one would calculate in inviscid approximation, provided that in the inviscid calculation one takes the quantity $R$ to be large, implicitly or explicitly. In other words, an inviscid calculation must provide for the return path of flow-generated currents through fixed conductors coplanar with the fluid elements generating the currents.

[9] J. Hartmann, Kgl. Danske Videnskab. Selskab Mat.-fys. Medd. **15**, 6 (1937); J. Hartmann and F. Lazarus, *ibid.* **15**, 7 (1937).

[10] J. A. Shercliff, Proc. Cambridge Phil. Soc. **49**, 136 (1953); **52**, 573 (1956); Proc. Roy. Soc. (London) **233**, 396 (1955); J. Fluid Mech. **1**, 644 (1956).

[11] W. Murgatroyd, Phil. Mag. **44**, 1348 (1953).

Such inviscid flow calculations have been performed by Donaldson[4,12] and by Fraenkel.[5]

The flows being considered here are at low magnetic Reynolds number. Perturbations of the magnetic field due to induced currents are not considered. However, the increased retardation of the flow due to a conducting region on the bottom illustrates the tendency of the lines of force to be frozen into the mercury and thus prevent relative motion. If one were to interpose an insulating surface between the mercury and the conducting region, there would be electric field components parallel to $H$ in the insulator, so that even if the bottom region had infinite conductivity, there could still be relative motion of the magnetic lines of force in the conductor and in the mercury.

Consideration of Eq. (6) suggests that in the case $R=0$, the insulated bottom, the flow for large $M$ is characterized by

$$c\mathbf{E}\times\mathbf{B}/B^2=-\mathbf{u}, \tag{15}$$

which is just the condition that pertains in a fluid of infinite conductivity where the lines of force are frozen into the fluid and move with the fluid velocity.[13] In the present case with viscous effects compressed into a thin layer the electric field induced is one which in the absence of nonmagnetohydrodynamic forces induction drag[13] would cause the flow to approach a velocity such that Eq. (15) is satisfied in a characteristic decay time

$$\tau_0=\rho c^2/(\sigma B^2)=1.31\times10^6/B^2 \text{ sec}. \tag{16}$$

This decay time is therefore characteristic of all flows for which Eq. (15) is not satisfied. Examples are flows with $R=\infty$ and irrotational wave motions. On the other hand, for rotational flows Eq. (15) can be satisfied and for large $M$ the characteristic decay time becomes

$$\tau_0'=M\tau_0=M[\rho c^2/(\sigma B^2)]. \tag{17}$$

The foregoing suggests that the mercury channel flows may also be characterized by the dimensionless quantity

$$N=(L/u)/\tau_0=(L/u)(\sigma B^2)/(\rho c^2),$$

discussed by Cowling[13] being of order unity. Here $L$ is a characteristic dimension in the flow direction, $u$ the flow velocity, and $\tau_0$ is defined in Eq. (16). The quantity $N$ is then a comparison of the time constants of the motion with and without a magnetic field.

Consider now the currents in the presence of an insulated and of an infinitely conducting bottom. In the former case one has $R=0$, and the total current induced in the fluid must vanish, i.e.,

$$\int_0^h (j_y)_f dz=0. \tag{18}$$

This leads to a current density distribution in which the total current in the boundary layer is equal and opposite to the total current in the slug flow. More precisely, for large $M$, $j_y$ has one polarity in the boundary layer, is zero at a depth determined from Eq. (11), viz.,

$$h'\cong(h\ln M)/M, \tag{19}$$

and is of opposite polarity in the slug flow. Clearly, one should expect effects associated with the thin Hartmann boundary layer, particularly if any sort of flow disturbance is introduced into the channel. In the limit of an infinitely conducting bottom, the field $E$ vanishes, the local current density becomes strictly proportional to the local fluid velocity, and all the induced current returns through the channel bottom, rather than through the Hartmann boundary layer. Hence flow disturbances in the presence of a conducting bottom depend less, if at all, on the fact that the fluid is viscous.

It is interesting to compare the fluid pressure gradient in the case when $R=0$ and $R=\infty$. One finds from Eq. (12) that for large $M$

$$\begin{aligned}(1/\rho)(\partial p/\partial x)&\cong-(\sigma_f B_z^2 u_0'/\rho c^2), && R=\infty,\\ &\cong-(\sigma_f B_z^2 u_0'/\rho c^2 M), && R=0.\end{aligned} \tag{20}$$

To achieve the same surface velocity at a given $M$ and $B_z$ over a conducting bottom of large $R$ requires a pressure gradient which is $M$ times the pressure gradient over an insulated bottom. Moreover, Eq. (20) suggests that the characteristic decay time for flow over an infinitely conducting bottom is that given by Eq. (17).

*Note added in proof.* It has come to our attention that C. C. Chang and T. S. Lundgren [*Heat Transfer and Fluid Mechanics Institute* (Stanford University Press, Stanford, California, 1959), p. 41] have calculated the flow through a rectangular duct of arbitrary conductivity with the walls parallel to the field displaced to infinity (generalizing the Hartmann case) and the flow through a finite duct with walls of infinite conductivity. In view of our Eq. (1), their results for walls of arbitrary conductivity can be rewritten to yield our free-surface channel flow analysis.

## CHANNEL FLOW EXPERIMENTS

Because only the surface of the mercury can be seen, one's impression of the channel flow is that it is fundamentally different from that on a conventional water table. To the extent that the mercury does not wet the insulated channel walls (we have used Lucite and glyptal-coated copper) when both are quite clean, or if the walls are not highly polished, so that they act as a source of capillary waves—with no field the mercury surface is covered with a fine pattern of intersecting capillaries—much like Mach lines. The intensity of such waves increases with increasing surface velocity and decreases with increasing applied field. It has actually proved advantageous to work with unclean mercury and chan-

[12] In reference 4 Donaldson considers inviscid flow in an insulated channel with walls of a laminated insulator-conductor construction. This construction is suggested to ensure current return in conductors coplanar to the current-generating fluid elements.

[13] T. G. Cowling, *Magnetohydrodynamics* (Interscience Publishers, Inc., New York, 1957), p. 11.

nel surfaces to ensure that there is no slip at boundaries and to suppress capillary disturbances. Thus far we have seen no evidence of boundary layer phenomena or flow instabilities in the absence of a magnetic field, in regimes where occurrence might have been expected from shallow water flow instability studies.[14] Flashes and irregularities such as might arise with the onset of turbulence would be hard to see in the presence of the capillary patterns. Moreover, we have not measured volume flow rates as would be required to compare the delay by a magnetic field of the onset of turbulence with what one might expect from closed channel studies.[15] Under all conditions in which experiments have been run, no evidence has been found of flow choking due to boundary layer growth.

The first group of experiments to be described involved surveys of the depth, surface velocity, and electric potential in a slightly divergent insulated channel. Figure 2 shows a potential survey in a completely insulated channel where the gradients in the $y$ or across-the-channel direction agree satisfactorily with what one would predict from Eq. (6). The flow is one-dimensional to a good approximation through all of the uniform magnetic field region. By contrast consider Fig. 3 in which the channel with the same geometry as in Fig. 2 was used as a power generator by connecting externally two short wall electrodes. The effect of allowing conduction to an external circuit is the same as though the flow had encountered a local region of conducting bottom. Along the line between electrodes, the potential gradient [see Eq. (6)] is reduced. A comparison of the potential gradients across the channel at the electrode position in Figs. 2 and 3 enables one to estimate the equivalent $R$ in Eq. (6), assuming velocities in the two cases are the same. The reduction in $E$ observed is as though there were a copper conducting region across the channel about 0.02 cm thick. Since the increased pressure gradient called for by Eq. (14) is not available, there is a pileup and a hydraulic jump is formed. The flow is no longer one-dimensional. Figures 4 and 5 show measurements of depth and flow velocity along the centerline of the channel. The effect of extracting power from the channel shows quite vividly here. In cases $D$ and $E$ the channel side walls were conducting, with an external connection across a small resistance in case $E$, whereas in case $D$ no external connection was made (current return paths through the mercury both in and outside the magnetic field were no longer one-dimensional). In both cases the flow behaved as though it were running through a conducting channel, with current return in the boundary layer being of little consequence. In case $D$ the flow is "choked" at the field entrance, with a hydraulic jump appearing.

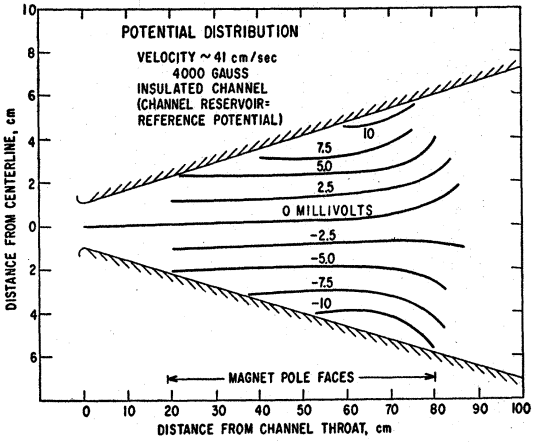


FIG. 2. Survey of electric potential in free-surface mercury flow, in a completely insulated channel (case $B$, Figs. 3 and 4). Note horizontal scale contraction.

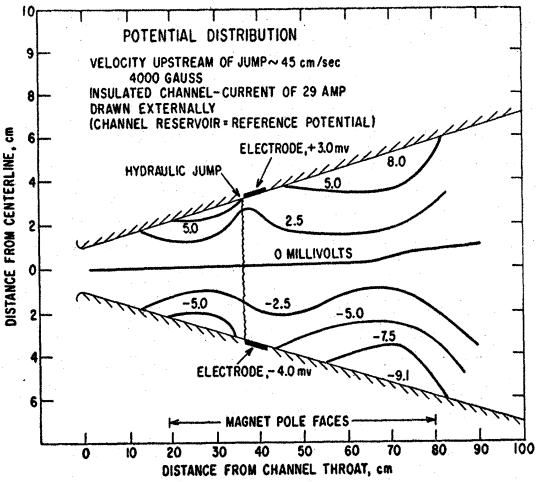


FIG. 3. Survey of electric potential in free-surface mercury flow in a channel insulated except for short wall electrodes through which power is extracted (case $C$, Figs. 3 and 4). Note horizontal scale contraction.

Two further experiments of interest were the follow-

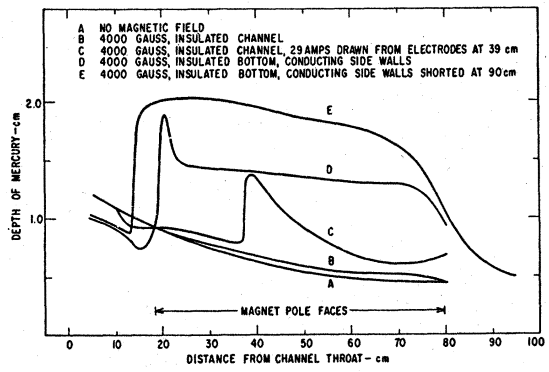


FIG. 4. Surveys of mercury depth in free-surface channel flow in a variety of experimental situations. Note the hydraulic jumps in $C$ and $D$, the former at the locus of power extraction, the latter representing a "choked" flow condition.

[14] A. M. Binnie, J. Fluid Mech. **5**, 561 (1959).
[15] R. C. Lock, Proc. Roy. Soc. (London) **A233**, 105 (1955).

ing: A strip of copper, thin compared to the fluid depth, was mounted along the $y$ direction in the channel, first on the bottom and up the walls to the mercury surface and, alternatively, starting at the walls on the channel bottom and running up and then across the channel, but not in contact with the mercury surface—a bridge, as it were. As expected, and as illustrated in Fig. 6, the flow effect is the same. A small hydraulic jump forms over/under the copper, and the potential gradient shows the reduction expected from Eq. (6). In a second experiment a copper disk which was very thin compared to the fluid depth was mounted on the bottom. With both subsonic and supersonic flow (with respect to surface wave velocity) through the magnetic field the gross effect due to change in $E$ and $\partial p/\partial x$ over the disk was nearly as though a fixed cylinder were immersed in the flow. Most striking was the formation of a Karman vortex street in the wake of the disk (see Fig. 7). When we replaced the strip or disk by insulating material of the same geometry, all effects vanished. Moreover, so long as the strip or disk was thin compared to the fluid depth, there was no difference between observations with the obstacle on the channel bottom or inset to be flush with the bottom.

As one would expect, it is quite easy to accelerate or decelerate the channel flow by applying a small voltage to electrodes arranged as in Fig. 3. A few millivolts can, with one polarity, so decelerate the flow as to form an hydraulic jump with mercury flowing over the side walls, while opposite polarity can so accelerate the flow as to cause the mercury to separate in the electrode region. Finally if short segments of conductor are formed by chopping the mercury flow mechanically, the segments can be accelerated roughly as an entity on passing by the electrodes with a suitable potential. No quantitative studies of these phenomena have as yet been carried out, theoretically or experimentally.

In the region of entry into and exit from the magnetic field, the channel surface shows in terms of a locally increased depth the additional pressure gradient one would expect in the nonuniform field region. We have not made any studies of this beyond what is shown in Figs. 4 and 5. Qualitatively the behavior is in agreement with the predictions of Hartmann[9] and Shercliff[10] who have considered the entry and exit problem in some detail for closed channels.

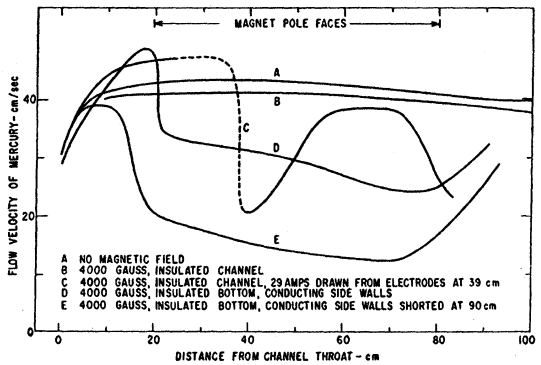


FIG. 5. Surveys of surface velocity in free-surface channel flow. Note particularly the effects on entry into and exit from the field.

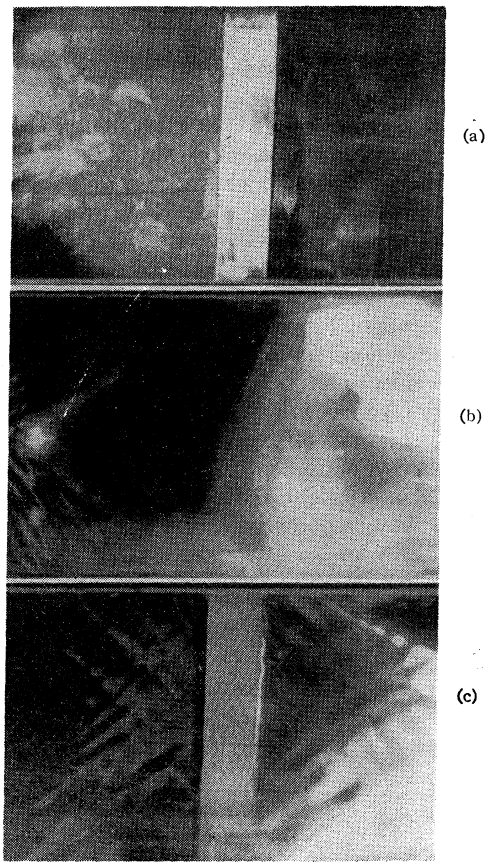


FIG. 6. Disturbance in channel flow over a conducting region. A 1-cm wide 0.013-cm thick copper strip on the channel bottom is transverse to the flow direction in (a). The strip also comes up the channel walls to above the mercury surface. The view is normal to the channel surface via a 45° mirror. In (b) mercury is flowing through 4200 gauss; an hydraulic jump has formed over the strip. In (c) the strip is inverted so that it contacts the mercury at the walls but is above the surface elsewhere. A hydraulic jump is formed on the mercury beneath the strip indistinguishable from (b). Flow velocity is ~40 cm/sec, depth ~1 cm.

## SURFACE WAVE MOTION

We have alluded in the foregoing to flows being subsonic or supersonic with respect to surface wave velocity, in the sense of regarding surface wave velocity as a characteristic or "sound" velocity in the channel. Let us examine the propagation of small-amplitude disturbances in shallow mercury in greater detail. The propagation characteristics may be expected to depend on gravity and surface tension,[16,17] with viscosity and

[16] H. Lamb, *Hydrodynamics* (Dover Publications, Inc., New York, 1945).

[17] A. H. Taub in *Handbook of Physics*, E. U. Condon and H. Odishaw, Editors (McGraw-Hill Book Company, Inc., New York, 1958), pp. 3–55; or J. J. Stoker, *Water Waves* (Interscience Publications, Inc., New York, 1957).

magnetohydrodynamic effects providing attenuation. It is not difficult to include viscosity and surface tension, but they play a trivial role in mercury, numerically speaking, so that we shall ignore them in this paper. (Capillaries do have a profound effect on the appearance of such surface disturbances as the classical "fish-line" pattern.[16]) Surface waves are of interest not only in terms of understanding the channel disturbances one sees, but also because the velocity of gravity waves plays the role of the velocity of sound in the usual hydraulic analogy.

The result desired follows from the equations of shallow water theory for propagation of small disturbances in one dimension (no viscosity or surface tension),[16] viz.,

$$\partial u/\partial t = -g(\partial \eta/\partial x)+X, \tag{21a}$$

and

$$\partial \eta/\partial t = -(\partial/\partial x)(h_0 u), \tag{21b}$$

where the fluid is basically at rest, $u=u(x)$ is the fluid velocity associated with the disturbance, $\eta=\eta(x)$ is the surface displacement from the undisturbed depth $h_0$ (which we take not to vary in the propagation direction but which may vary in the $y$ or across-the-channel direction, as discussed later), and $X$ is the body force which here is the Lorentz force term for wave propagation transverse to a magnetic field $B_z$, viz.,

$$X = -\sigma u B_z^2/(\rho c^2). \tag{22}$$

In arriving at Eq. (19) one assumes nonlinear terms are small, pressure everywhere in the fluid is hydrostatic, and vertical accelerations are neglected so that $u=u(x)$ only. Equations (21) and (22) combine to yield the following irrotational wave equation for $u$ or $\eta$ in a horizontal channel of mean depth $h_0$[18]:

$$\begin{aligned}\partial^2 u/\partial t^2 &= gh_0(\partial^2 u/\partial x^2) - (\sigma B_z^2/\rho c^2)(\partial u/\partial t)\\ &= v_0^2(\partial^2 u/\partial x^2) - (1/\tau_0)(\partial u/\partial t),\end{aligned} \tag{23}$$

where $\tau_0$ is the characteristic time defined in Eq. (16) and $v_0$ is the classical gravity wave velocity.[16] From Eq. (23) one finds the phase velocity for a wave of angular frequency $\omega$ to be

$$v = (2)^{\frac{1}{2}} v_0 \{1+[1+(1/\omega\tau_0)^2]^{\frac{1}{2}}\}^{-\frac{1}{2}} \text{ cm/sec}, \tag{24}$$

and the attenuation constant to be

$$\alpha = [(2)^{-\frac{1}{2}}\omega/v_0]\{-1+[1+(1/\omega\tau_0)^2]^{\frac{1}{2}}\}^{\frac{1}{2}} \text{ cm}^{-1}. \tag{25}$$

Note that $v_0\tau_0$ plays the role of a "characteristic" distance; for an $h_0$ of 1 cm and $B_0$ of 4000 gauss, $v_0\tau_0=2.5$ cm. Equations (24) and (25) are plotted in Fig. 8 for these values of $h_0$ and $B_0$. A generalization in two dimensions of the foregoing irrotational wave equation is discussed in Appendix A.

In addition to Donaldson, Lundquist[6] and Fraenkel[5] have considered surface wave velocity. Lundquist obtains a result in the case of infinite conductivity, a

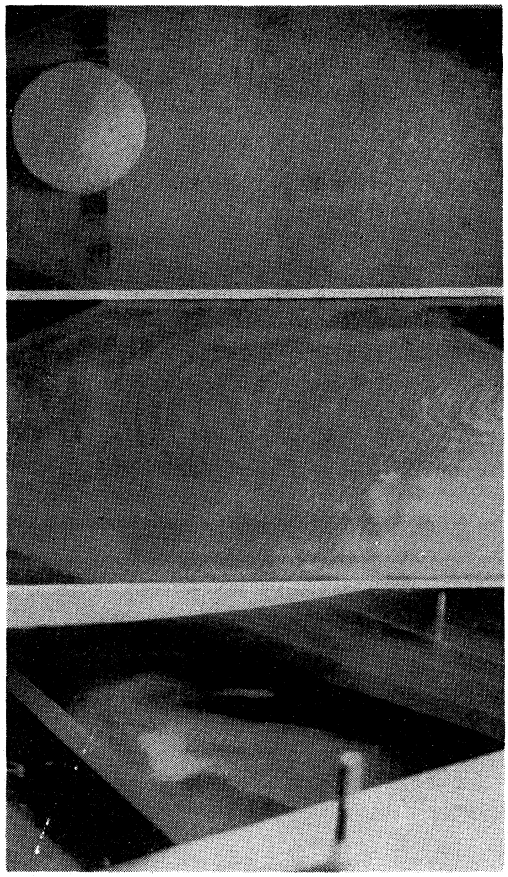


FIG. 7. In (a) is seen a 2-cm radius copper disk, 0.013 cm thick, on the channel bottom—the view being as in Fig. 6. In (b) surface dirt shows the magnetohydrodynamic effect of a low-velocity flow over the disk at 4200 gauss. In (c) one has a view of the channel flow over the disk while looking upstream. The velocity is such that the disk is shedding a vortex street.

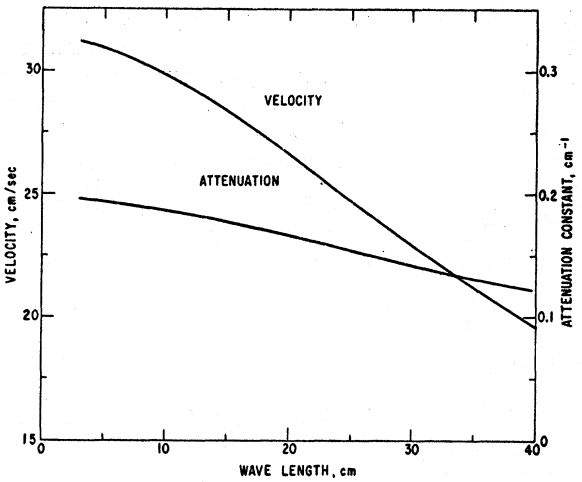


FIG. 8. Velocity and attenuation of gravity waves vs wavelength in mercury at 4000 gauss—shallow-liquid approximation, depth 1 cm.

[18] C. duP. Donaldson, reference 4, and L. H. Fraenkel, reference 5, also arrived at this equation.

situation which does not apply to the present work since the approximations of this paper include a small magnetic Reynolds number. Fraenkel's excellent survey of some of the basic problems of shallow-liquid magnetohydrodynamics includes both the result obtained in Eq. (22) and the generalization in Appendix A.

As an examination of Fig. 8 indicates, it is only for extremely low-frequency waves that a velocity significantly different from $(gh_0)^{\frac{1}{2}}$ can be expected at 4000 gauss. We have attempted to detect a deviation in two ways. In a steady channel flow of known depth, surface fluid velocity in excess of $(gh_0)^{\frac{1}{2}}$ was measured by an impact probe, by potential measurement and by a paddle wheel arrangement with tips immersed in the fluid. Then a standing wave was formed by creating a small surface disturbance. It would seem reasonable that with viscous effects in the channel flow confined to the thin boundary layer, a superimposed surface disturbance might well behave as though the flow were inviscid. Hence no correction would be needed in applying Eqs. (24) and (25) to this experiment. Within our accuracy of measurement, admittedly crude, the "Mach angle" of the standing wave (with respect to surface velocity measured) was independent of magnetic field. At points on the wave well away from the disturbance the wave profile was slightly broadened. This may have been due to a slightly lower velocity for low frequency waves, a much greater attenuation for high frequency waves, or an interaction with the ever-present capillaries (despite their diminution in a magnetic field).[7]

A second experiment involved the production of traveling waves in a rectangular trough of mercury otherwise at rest. No quantitative data are offered beyond the observation that at 4200 gauss, using a "pebble dropping" technique, we could not create a disturbance which would survive to the edges of the trough (a 10-cm path). A nearly one-dimensional disturbance of appreciable amplitude propagating from one end of the trough decayed so rapidly that within several centimeters of the disturbance origin one saw only a disturbance whose wavelength was of the order of the trough dimension (30 or 40 cm).

With regard to the existence of a magnetohydraulic analogy, the free-surface mercury channel flow is indeed a true analogy to two-dimensional compressible flows which are normal to the magnetic field direction and independent of the coordinate in the field direction. Although the direction of the magnetic field must be everywhere the same, the magnitude of the field can depend on the coordinates perpendicular to the field. In this case one would have to ignore the fact that a three-dimensional field configuration necessarily has components, albeit small, normal to the main field direction. It may in some circumstances nevertheless be legitimate to ignore these components.

In linear approximation one can show an analogy between the descriptive equations of the channel and of the gas regardless of the dependence of gas conductivity on density and for any specific heat ratio. Nonlinear effects in the mercury channel simulate the nonlinear behavior of a gas in which the conductivity is proportional to density and the pressure is proportional to the square of the density, i.e., a specific heat ratio of two. The requirement on conductivity follows from the fact that for the gas we must have

$$\nabla\times\mathbf{E}=0, \tag{26}$$

and

$$\nabla\cdot\mathbf{j}=0, \tag{27}$$

where $\mathbf{j}$ is the current density and $\mathbf{E}$ is required to be perpendicular to $\mathbf{B}$. In the free-surface mercury channel, $\mathbf{E}$ must be parallel to the mercury surface and hence perpendicular to $\mathbf{B}$ if $\nabla h$ is small compared to unity. (This last condition on $\nabla h$ is required in the conventional hydraulic analogy. However, as in the conventional hydraulic analogy the onset of shocks can be studied as the onset of hydraulic jumps, since weak shocks are nearly isentropic.) Moreover, we require in the channel

$$\nabla\cdot(\mathbf{j}h)=\nabla\cdot\mathbf{J}=0, \tag{28}$$

where $\mathbf{j}$ is the projection of the current density vector on the plane of the table. Thus the condition for the channel on $\nabla\times\mathbf{E}$ becomes

$$\nabla\times[(\mathbf{J}/\sigma_0 h)+(\mathbf{u}\times\mathbf{B}/c)]=0. \tag{29}$$

Hence $\sigma_0 h$ in the channel is the analog of $\sigma$ in the gas. Note that the identification of $\mathbf{j}h$ in the channel with $\mathbf{j}$ in the gas is necessary to maintain formal identity in the equations of motion. Moreover, we have not used the Maxwell equation $\nabla\cdot\mathbf{E}=4\pi q$, where $q$ is charge density, in either the gas or channel description, for we have not been interested in charge density and the force due to charges is small here as in the usual magnetohydrodynamic equations.

In the case of two-dimensional unsteady flows in a fluid of infinite conductivity Blank and Grad[19] have shown that the defining magnetohydrodynamic equations may be so cast as to render them formally equivalent to conventional fluid dynamic equations.

In our consideration of the analogy problem, we examined the question of altering the analogy specific heat ratio by working with other than a rectangular channel. Kelland[20] found the propagation velocity of long waves in a shallow horizontal channel of arbitrary cross section symmetrical about a center line to be $(g\bar{h}_0)^{\frac{1}{2}}$, where $\bar{h}_0$ is the mean depth of the half-channel width. Some authors[21] have suggested that if the channel profile were of the form $z=y^n$, then the analog specific

[19] A. A. Blank and H. Grad, New York University Institute of Mathematical Sciences, Research and Development Rept., U. S. Atomic Energy Commission Computing and Applied Math. Center, NYO-6486 (July 15, 1958).

[20] P. Kelland, Proc. Roy. Soc. Edinburgh **14**, 497 (1840); work quite fully described in reference 15.

[21] The most recent discussion of this problem is by W. H. T. Loh, J. Aero/Space Sci. **26**, 389 (1959).

heat ratio would be a function of $n$ and therefore adjustable to values other than two. There are some theoretical questions involving the consistency of such arguments with the assumptions of shallow-water theory (the assumption of no vertical accelerations is difficult near the edges of a shallow triangular channel, for example).[22] We constructed a series of very shallow channels and could find no effect within measurement accuracy of profile on measured wave velocities at the channel center. With the exception of the rectangular channel, so long as the channels were shallow, channel edge effects such as are fully discussed in Lamb[16] completely dominated the wave motions and rendered them no longer one-dimensional.

We have examined the flow modifications caused in the mercury channel by such bodies as wedges and cylinders. The surface wave disturbances are in no essential way different from those one would observe on a water table in terms of hydraulic jumps simulating shock waves, wake flows shedding vortices, etc., all under conditions one would expect for the flow velocities used in terms of the gravity wave velocity. One major difference is the effect already mentioned of conducting regions placed on the channel bottom which cause disturbances as though they were solid bodies in the flow. A second major difference, on the one hand, is the enhancement of visibility of capillary effects in mercury as compared to water ($T/\rho = 74$ in water, 40 in mercury) due to their lower velocity, and, on the other hand, the striking attenuation of capillary waves by the magnetic field. One finds that capillaries associated with unsteady disturbances of the mercury surface in a magnetic field are damped almost critically. This is qualitatively consistent with Shirokov's conclusion[7] that capillaries are critically damped in a fluid of infinite conductivity. In a steady surface disturbance in channel flow, such as the classical "fish-line" disturbance[16] at flow velocities in excess of $(gh_0)^{\frac{1}{2}}$ but less than the group velocity of capillaries one finds a beautiful pattern of capillaries ahead of the hydraulic jump (see Fig. 9 and Appendix A). We do not discuss this work further here since the pattern is virtually unchanged over the magnetic field range available to us—there is some barely noticeable attenuation of the capillaries and broadening of the main jump with increasing distance from the disturbance center line.

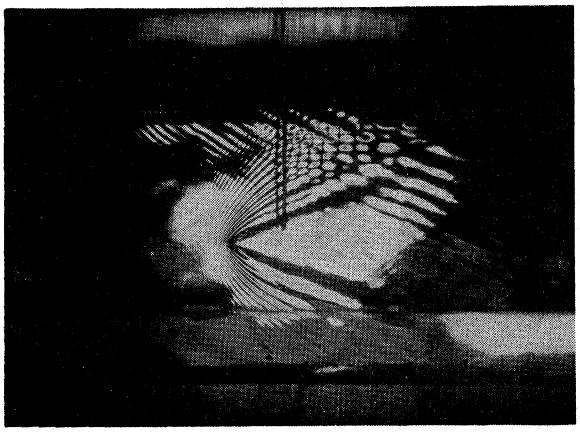

FIG. 9. Disturbance created in "supersonic" mercury flow by a small wire touching the mercury surface; field is 4200 gauss—the pattern at 0 gauss differs only subtly.

[22] E. V. Laitone [Bull. Am. Phys. Soc. Ser. II, 5, 43 (1960)] has raised questions about the nonrectangular channel also.

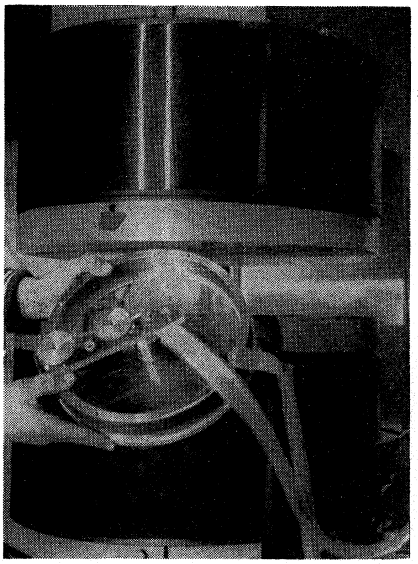

FIG. 10. Photograph of the free-surface mercury motor—over-all diam 10 in.

## ROTATING FLOWS

As already mentioned, well-defined vortices are produced in the wakes of cylinders and conducting spots in the mercury channel flows; extensive vortices can be produced by disturbing an otherwise stationary trough of mercury. The apparent stability of these vortices formed with the vorticity vector in the field direction impressed us sufficiently that we sought to study the decay of such flows from a "standard" initial state. To obtain such a state we have used a free-surface mercury motor as illustrated in Fig. 10. The motor has a Lucite bottom, an inner copper cylindrical stator or electrode of radius 2.2 cm, and an outer copper electrode of radius 12.5 cm. The equilibrium mercury depth was 1.9 cm. The mercury was brought up to a steady-state rotation by placing the motor between our magnet polepieces and applying between 5 and 35 mv across the electrodes, depending on the applied field. Once a steady state was reached, the driving voltage was disconnected and the decay observed by measuring either the voltage drop across the electrodes or by following the potential on a probe touching the mercury surface (a radial location of minimum depth change being selected). No essential difference was noted between these two measurement points. The device has several interesting

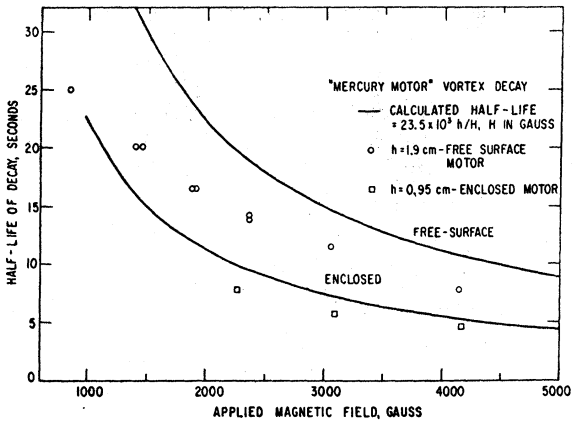


FIG. 11. Comparison of calculated and observed half-lives for decay of vortex flow in free-surface and closed-surface mercury motors (hydromagnetic capacitors). The half-life of the initial decay period during which the Hartmann-type flow is being established is of the order of 5 to 10 sec, with little or no dependence on the applied magnetic field.

properties as a motor, one being the surface profile, another being its self-regulating nature. If the driving voltage is too high, the mercury breaks away from the central stator and breaks the exciting circuit.

That one can establish a slowly decaying rotating flow of this type indicates that the boundary layer must be of nearly constant thickness in the flow direction at a given radius. This is just the case with a Hartmann boundary layer, and in fact it is reasonable to suppose that this characterizes the decaying flow. The dissipation of such a flow must then be the result of viscous drag in the boundary layer and of induction drag in the slug or free stream flow. Moreover, the velocity change in the decaying flow should be observable as a potential decay, the two being proportional to one another through Eq. (6).

A time constant for the decaying flow can be most simply obtained as follows. In the presence of viscous drag and induction drag only, the decay of velocity is

$$\rho\partial u_0/\partial t = -(j_r B_z/c) + \mu\nabla^2 u. \tag{30}$$

Integrating with respect to depth and dividing through by $u_0'\rho h$ yields approximately

$$\frac{1}{u_0'}\frac{du_0'}{dt} \cong \frac{-B_z}{\rho h c u_0'}\int_0^h j_r dz + \frac{\nu}{h u_0'}\int_0^h \frac{\partial^2 u}{\partial z^2}dz. \tag{31}$$

On substituting for $j_r$ from Eq. (11), for $E$ from Eq. (6), and for $u$ from Eq. (3), and performing the indicated integrations, one finds the first term vanishes (total current in the fluid is zero), and for large $M$ one is left with

$$(1/u_0')(du_0'/dt) \cong (-\nu M/h^2) = -(1/M\tau_0). \tag{32}$$

This result also can be obtained from a generalized vorticity analysis (see Appendix B).

Half-lives for decay computed from Eq. (32) are compared with measured half-lives in Fig. 11. The decay measurements were complicated by the fact, not immediately recognized, that it should take some time for a Hartmann boundary layer with zero net current in the fluid to become established after removal of the driving current. When the decaying flow was followed for a time longer than several of the half-lives predicted by theory, a change in the decay to the final values plotted in Fig. 11 was observed consistently. Some of the difference between theory and experiment here may lie in dissipation neglected at the inner and outer walls of the motor. Changes of surface deformation are not put in the calculation, but it must be noted that by the time the motor has decayed through several half-lives to the time of measurement, the surface profile has flattened to a point where the motor had essentially a constant depth.

The mercury motor is nearly equivalent to a hydromagnetic capacitor, a device of recent interest.[23] The difference lies in that some energy is stored in the free-surface motor as potential energy of deformation of the mercury surface, whereas in the true hydromagnetic capacitor all the energy storage is kinetic. One can then interpret Fig. 11 in terms of the decay of this "mercury motor" capacitor on open circuit, i.e., this, as all hydromagnetic capacitors, has a leaky dielectric.

As this work was being prepared, a paper of Chang and Lundgren[24] appeared in which the properties of a "mercury motor" which is completely enclosed are calculated, i.e., the free-surface condition is replaced by an insulated top cover. One finds their calculated charging time constant should be the same as the decay constant, Eq. (32), providing that the characteristic depth in the closed case be taken as half the actual depth, since the top of the motor also has a Hartmann boundary layer. Chang and Lundgren also neglect dissipative effects at the walls parallel to the applied field. It was a relatively simple matter to enclose our mercury motor, making it identical to the geometry studied by Chang and Lundgren, and the results of a series of decay measurements are given in Fig. 11. A calculated quantity which is easy to check is the resistance of the motor when running at steady-state —our measurements agree within experimental error with their theoretical result.

## CONCLUDING REMARKS

The work reported here shows that the free-surface mercury channel has pedagogical value in understanding flows in which the magnetic Reynolds number is low and the dimensionless parameter $N = (L/u)/\tau_0$ is of order unity. Moreover, there is the possibility of obtaining semiquantitative data by using the channel as a magnetohydraulic analogy. While the principal application of the analogy may well be to simulation of closed

[23] O. Atkinson, W. R. Baker, A. Bratenahl, H. P. Furth, and W. B. Kunkel, J. Appl. Phys. **30**, 188 (1959).
[24] C. C. Chang and T. S. Lundgren, Phys. Fluids **2**, 627 (1959).

channel flows at low magnetic Reynolds numbers, there are undoubtedly special geometries for which the channel may provide useful insight into the flows around bodies in the presence of a magnetic field. Finally, the work already done suggests other experiments in linear and rotating flows which should be interesting in the context of the shallow-liquid approximation.


### ACKNOWLEDGMENTS

The impetus and support of A. J. Nerad in this work is gratefully acknowledged. Discussions with C. Muckenfuss and other colleagues have been most helpful as have comments on the manuscript by L. H. Fraenkel. The assistance of E. C. Bigelow, K. H. Cary, and L. Osburg has been invaluable.


## APPENDIX A

### Wave Equation for Irrotational Flow

We have developed the wave equation which governs two-dimensional irrotational surface waves in the presence of a uniform magnetic field under the usual water table approximations. Specifically, we assume that the flow velocity, current density,[25] and pressure gradient are independent of depth, and we neglect surface tension and all nonlinear terms.

Under these approximations the equation of motion for the two-dimensional velocity vector $\mathbf{u}$ has the form

$$\rho\partial\mathbf{u}/\partial t=-\rho g\nabla h+(\mathbf{j}\times\mathbf{B}_z/c)-\nabla p_0. \tag{A1}$$

Here $\rho$ is the fluid density, $h$ is the local thickness of the fluid layer which has the equilibrium value $h_0$, $\mathbf{j}$ is the current density, and $p_0$ is the pressure applied to the top surface of the fluid. The term $p_0$ is included to make possible the study of the effects of certain types of external perturbation on the flow field.[26]

We express the two-dimensional velocity and current density vectors in terms of the scalar functions $\psi$ and $\chi$ by means of the equations

$$\mathbf{u}=\nabla\psi, \tag{A2}$$

$$\mathbf{j}=\nabla\times\mathbf{k}\chi. \tag{A3}$$

(Here $\mathbf{k}$ is a unit vector normal to the flow plane and parallel to the applied magnetic field.)

The equation of motion then assumes the form

$$\rho\nabla\partial\psi/\partial t=-g\rho\nabla h-\nabla p_0-(B/c)\nabla\chi. \tag{A4}$$

The linearized form of the continuity equation is

$$\partial h/\partial t=-h_0\nabla\cdot\mathbf{u}=-h_0\nabla^2\psi. \tag{A5}$$

(Here $\nabla^2$ is the two-dimensional Laplacian operator). In view of Eq. (A5) the divergence of Eq. (A4) is

$$-(\rho/h_0)(\partial^2h/\partial t^2)=-g\rho\nabla^2h-\nabla^2p_0-(B/c)\nabla^2\chi. \tag{A6}$$

Since the magnetic field is time independent, the electric field may be expressed in terms of a scalar potential, to wit,

$$\mathbf{E}=-\nabla\varphi. \tag{A7}$$

Hence

$$\mathbf{j}=\nabla\times\mathbf{k}\chi=-\sigma[\nabla\varphi+(\mathbf{B}\times\nabla\psi/c)]. \tag{A8}$$

The curl of Eq. (A8) has the form [using Eq. (A5)]

$$\nabla^2\chi=(\sigma|B|/c)\nabla^2\psi=-(\sigma|B|/h_0c)(\partial h/\partial t). \tag{A9}$$

Hence Eq. (A6) has the form

$$\partial^2h/\partial t^2-gh_0\nabla^2h+(\sigma B^2/\rho c^2)(\partial h/\partial t)=h_0\nabla^2p_0/\rho. \tag{A10}$$

This equation is equivalent to Eq. (23) in the text. It contains the characteristic velocity

$$v_0=(gh_0)^{\frac{1}{2}}, \tag{A11}$$

the characteristic distance

$$x_0=v_0\rho c^2/(\sigma B^2), \tag{A12}$$

and the characteristic time

$$\tau_0=x_0/v_0. \tag{A13}$$

If the units of time and space are set equal to $\tau_0$ and $x_0$, respectively, Eq. (A10) assumes the form

$$\partial^2h/\partial t^2-\nabla^2h+\partial h/\partial t=(1/\rho g)\nabla^2p_0. \tag{A14}$$

In studying the qualitative effects of a perturbation which moves with respect to the fluid at a uniform velocity, it is useful to have the Green's function which is a solution of the equation[27]

$$\frac{\partial^2h_m}{\partial t^2}-\frac{\partial^2h_m}{\partial x^2}-\frac{\partial^2h_m}{\partial y^2}+\frac{\partial h_m}{\partial t}=\delta(x+mt,y). \tag{A15}$$

Here $m$ is the Mach number of the perturbation which is moving in the negative $x$ direction, i.e., the perturbation velocity is $mv_0$.

The form of the solution depends upon whether $m$ is less than, equal to, or greater than unity.[28]

If $m$ is less than unity,

$$h_m=[1/2\pi(1-m^2)^{\frac{1}{2}}]K_0(\kappa^+\rho^+)\exp[\kappa^+(x+mt)],$$

where

$$\kappa^+=m/[2(1-m^2)] \tag{A16}$$

and

$$\rho^+=[(x+mt)^2+(1-m^2)y^2]^{\frac{1}{2}}.$$

[25] Since the electric field is not in general equal to $\mathbf{B}\times\mathbf{u}/c$, where $\mathbf{u}$ is the free-stream velocity, the current density in the free stream is comparable to that in the boundary layer. Hence it is legitimate to neglect the boundary layer current on the basis of the usual water table assumption that thick boundary layers do not develop since the viscosity is small.

[26] In reference 5, Fraenkel considers the propagation of the disturbance from a perturbation which does not move with respect to the fluid.

[27] This differential equation is discussed by P. M. Morse and H. Feshbach, [*Methods of Theoretical Physics* (McGraw-Hill Book Company, Inc., New York, 1953), Sec. 7.4, p. 865 ff] in connection with heat transmission through an absorbing gas. The Green's functions given here are appropriate integrals of the two-dimensional Green's functions given by these authors in Eq. (7.4.27).

[28] The Bessel functions $I_0$ and $K_0$ are used with normalization defined by E. T. Whittaker and G. N. Watson, *Modern Analysis* (Cambridge University Press, New York, 1940), p. 372 ff.

If $m$ is equal to unity,

$$h_1=[4\pi(x+t)]^{-\frac{1}{2}}\exp\{-y^2/[4(x+t)]\}. \quad \text{(A17)}$$

If $m$ is greater than unity,

$$h_m=0 \quad \text{for} \quad x+mt<(m^2-1)^{\frac{1}{2}}|y|,$$
$$h_m=\tfrac{1}{2}(m^2-1)^{-\frac{1}{2}}I_0(\kappa^-\rho^-)\exp[-\kappa^-(x+mt)] \quad \text{(A18)}$$
$$\text{for} \quad x+mt>(m^2-1)^{\frac{1}{2}}|y|,$$

where

$$\kappa^-=m/[2(m^2-1)],$$

and

$$\rho^-=[(x+mt)^2-(m^2-1)y^2]^{\frac{1}{2}}.$$

The flow pattern which results from a highly localized pressure applied at a position which moves with respect to the fluid at a velocity $mv_0$ would be formally obtained by taking the Laplacian of the solutions given in Eqs. (A16)–(A18). If $m$ is greater than unity, the corresponding disturbance is concentrated along the Mach line because of the discontinuity in $h_m$ along this line.

In a physical case the form of the solution on the Mach line depends on the detailed shape of the pressure disturbance. It should be kept in mind that since the water table approximation breaks down for wavelengths which are comparable to or smaller than the depth of the fluid, the solutions of Eq. (A10) for a delta-function pressure disturbance have quantitative physical significance only in the sense that they can be used as the Green's functions for constructing solutions for less localized disturbances. For example, if the pressure perturbation $p_0$ extends over a radius $r_0$ which is large compared to $h_0$ but small compared to $x_0$ the actual solutions are closely related to the Laplacian of the Green's functions. The behavior of the actual solutions along the Mach line depends, however, in detail on the shape of the pressure disturbance. The specific relationship for a disturbance with circular symmetry is

$$h(\mathbf{r},t)=\frac{1}{\rho g}\nabla^2\int h_m(|\mathbf{r}-\mathbf{r}'|,t)p_0(\mathbf{r}')d\mathbf{r}', \quad \text{(A19)}$$

where the components of the vectors $\mathbf{r}$ and $\mathbf{r}'$ are, respectively, $(x,y)$ and $(x'+mt, y')$.

Another complicating feature is that the appearance of the mercury surface in the presence of a localized disturbance is strongly affected by capillary waves which are not included in the foregoing analysis. Hence, although the expected lack of dependence of Mach angle on magnetic field strength has been qualitatively verified, a detailed comparison of the observed flow pattern with the solution of Eq. (A10) has not as yet been made.

## APPENDIX B

## Vortex Decay

We here consider a general two-dimensional rotational flow in the limit of large Hartmann number under the assumption that the variation of velocity with depth follows the Hartmann profile, and that the total fluid depth is always approximately equal to its undisturbed value, $h_0$. If $\mathbf{u}(x,z,t)$ is the free-stream velocity, for a closed contour, we find

$$\rho h_0\frac{d}{dt}\oint\mathbf{u}\cdot\mathbf{ds}=h_0\oint\mathbf{F}\cdot\mathbf{ds}. \quad \text{(B1)}$$

Here $h_0$ is the equilibrium mercury depth and $\mathbf{F}$ is the body force density, i.e.,

$$h_0\mathbf{F}=\mathbf{J}\times\mathbf{B}_z/c, \quad \text{(B2)}$$

where $\mathbf{J}$ is the free-stream current density integrated from the top of the boundary layer to the upper surface of the liquid. The pressure gradient term does not contribute to the right side of Eq. (B1). We ignore the difference between the actual local fluid depth, $h$, and the equilibrium depth, $h_0$. By using the fact that $\mathbf{B}_z$ is normal to the flow plane we may recast the right-hand side of Eq. (B1) so that the equation becomes

$$\rho h_0\frac{d}{dt}\oint\mathbf{u}\cdot\mathbf{ds}=-\frac{|B_z|}{c}\int\int dA\nabla\cdot\mathbf{J}, \quad \text{(B3)}$$

where the integral on the right is over the area enclosed by the contour and $\mathbf{B}_z$ is assumed to be directed in the positive sense with respect to the direction of contour integration. By charge conservation we have

$$\nabla\cdot\mathbf{J}=-\nabla\cdot\mathbf{J}_{\text{b.l.}}, \quad \text{(B4)}$$

where $\mathbf{J}_{\text{b.l.}}$ is the current density integrated over the boundary layer. For the Hartmann profile, we have

$$\mathbf{J}_{\text{b.l.}}\cong-(\rho\nu\sigma)^{\frac{1}{2}}\mathbf{u}_0\times\mathbf{B}_z/|B_z|. \quad \text{(B5)}$$

(The direction of the boundary layer current is such that the Lorentz force tends to drive the fluid in the direction of the free stream velocity.)

The substitution of Eqs. (B4) and (B5) into Eq. (B3) together with the use of Stokes' theorem then yields

$$\frac{d}{dt}\oint\mathbf{u}\cdot\mathbf{ds}=-\frac{|B_z|}{ch_0}\left(\frac{\sigma\nu}{\rho}\right)^{\frac{1}{2}}\oint\mathbf{u}\cdot\mathbf{ds}. \quad \text{(B6)}$$

Hence the vorticity decay constant is

$$(B_z/ch_0)(\sigma\nu/\rho)^{\frac{1}{2}}=1/(M\tau_0)=1/\tau_0', \quad \text{(B7)}$$

in agreement with the arguments in the text. It may be noted that Lehnert[29] has shown that the field-dependent portion of the decay factor for magneto-turbulence is a function of $\tau_0$, with the asymptotic state of the decay being two-dimensional with respect to the field.

[29] B. Lehnert, Quart. Appl. Math. 12, 321 (1955).

## DISCUSSION

Session Reporter: M. MITCHNER

**E. L. Resler, Jr.,** *Cornell University, Ithaca, New York:* Was the copper disk on the bottom flush or did it project into the flow and cause a disturbance?

**R. A. Alpher:** I showed one picture of just hydrodynamic flow over the disk and there is essentially no surface disturbance visible in the capillary pattern. We have also run experiments with disks in the bottom and therefore flush. The thickness of the copper we used is typically two hundreds of a centimeter.

**E. L. Resler, Jr.:** Is the disturbance due to the fact that the copper is anchoring the field lines, or is it due to an Alfvén mechanism which causes any disturbance to become cylindrical?

**B. Lehnert,** *Royal Institute of Technology, Stockholm, Sweden:* I think the lines are, in effect, anchored in the copper. By neglecting the influence of viscosity and for very strong magnetic fields, it is easily shown, in general, that the flow pattern become two-dimensional, in the sense that there should be the same state of flow along a magnetic field line.

For the case where the entire bottom surface of the channel is an insulator and when dissipation is neglected, the mercurcy next to the channel behaves in a manner equivalent to a free surface. The electric field induced by the flow across the magnetic field then becomes uniform in the direction of the latter and no currents flow in a stationary state. An analogy to this is a number of generators which all have the same electromotive force (corresponding to $\mathbf{v}\times\mathbf{B}$ with $\mathbf{v}$ and $\mathbf{B}$ constant) and which are connected in parallel.

Next, consider the alternative case where the entire surface of the channel is a perfect conductor and the electrical contact between the channel surface and the fluid layers above is excellent. Then, electric currents can *cross* the interface and this makes the channel surface form a part of the conducting fluid from the point of view of magnetohydrodynamic coupling. This also implies that there is a "fluid layer," i.e., the channel surface itself, where the fluid velocity is zero. If the fluid layers above moved, the situation would resemble that of a number of generators connected in parallel and where there is a short-circuit across the whole configuration caused by bottom of the channel. As a consequence, at high electrical conductivity and very strong magnetic fields, the flow adjusts itself so as not to induce infinite currents, i.e., the fluids are frozen to the bottom and stay at rest.

The case of a copper disk placed in the center of an insulated channel surface represents an intermediate situation where part of the channel surface is conducting and where both the magnetic field and conductivity are finite. Even if the copper plate is thin, the conductivity of copper is about 50 times larger than that of mercury, and some of the effects which I have outlined here still come into play.

**B. Lehnert:** In my experiment with a rotating conducting annulus at the bottom of a mercury layer, the analogy with frozen field lines applies. Field lines which are anchored in the annulus transmit their motion to fluid layers situated above. The parts of the conducting bottom which are at rest force the fluid on top of them to be at rest, somewhat like the situation in Dr. Alpher's experiments.

This question of anchored field lines is, of course, a way of expressing a thing which is much more complicated. In a more rigorous treatment one should look at the magnetic flux instead, and how this changes as the fluid moves.

**J. E. McCune,** *Aeronautical Research Associates, Princeton, New Jersey:* Is it not true, in fact, that there is no direct analogy, but only a similarity?

**R. A. Alpher:** There is a magnetohydrodynamic analogy in the same sense that one has an analogy for the usual compressible flow with a conventional water table. The analogy holds for low magnetic Reynolds number flows.

**E. L. Resler, Jr.:** I think the analogy is good as long as Joule heating is unimportant.

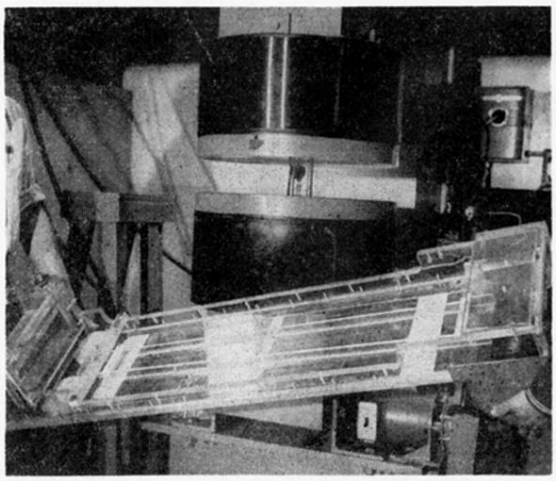

FIG. 1. Free-surface mercury channel is shown outside of the magnet gap for greater visibility. Copper strip and disk shown were used in experiments described in this paper.

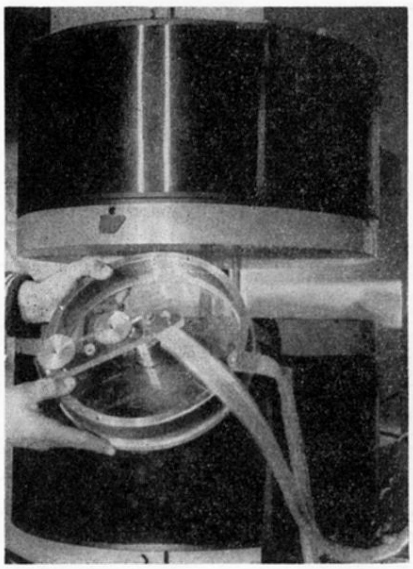

FIG. 10. Photograph of the free-surface mercury motor—over-all diam 10 in.

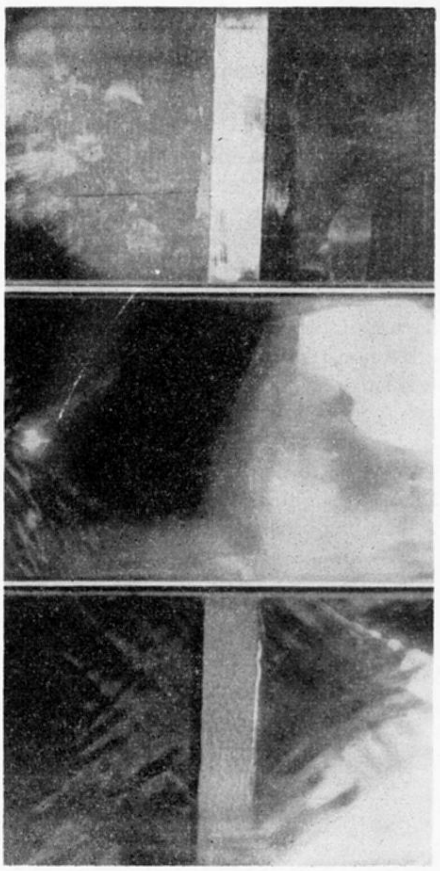


FIG. 6. Disturbance in channel flow over a conducting region. A 1-cm wide 0.013-cm thick copper strip on the channel bottom is transverse to the flow direction in (a). The strip also comes up the channel walls to above the mercury surface. The view is normal to the channel surface via a 45° mirror. In (b) mercury is flowing through 4200 gauss; an hydraulic jump has formed over the strip. In (c) the strip is inverted so that it contacts the mercury at the walls but is above the surface elsewhere. A hydraulic jump is formed on the mercury beneath the strip indistinguishable from (b). Flow velocity is $\sim$40 cm/sec, depth $\sim$1 cm.

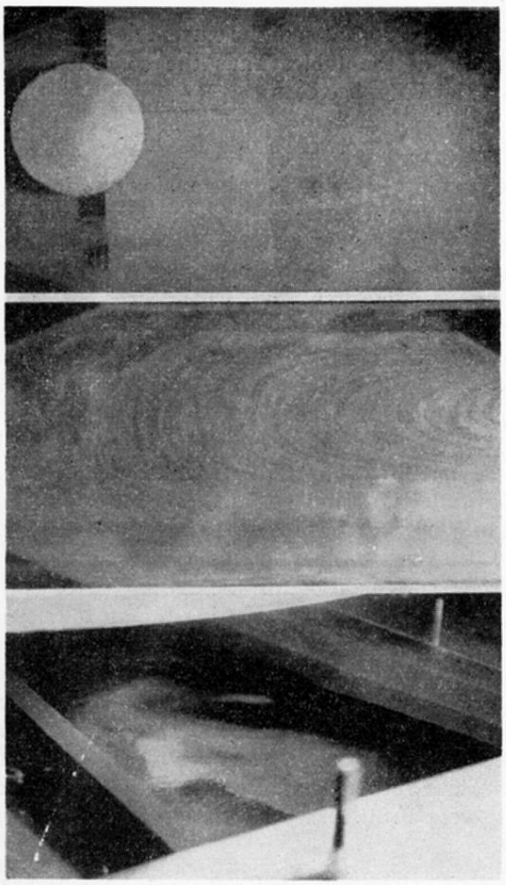


FIG. 7. In (a) is seen a 2-cm radius copper disk, 0.013 cm thick, on the channel bottom—the view being as in Fig. 6. In (b) surface dirt shows the magnetohydrodynamic effect of a low-velocity flow over the disk at 4200 gauss. In (c) one has a view of the channel flow over the disk while looking upstream. The velocity is such that the disk is shedding a vortex street.

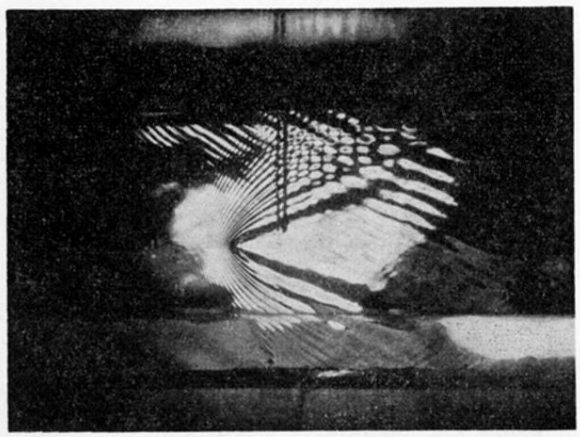

FIG. 9. Disturbance created in "supersonic" mercury flow by a small wire touching the mercury surface; field is 4200 gauss—the pattern at 0 gauss differs only subtly.